Metabologia (2026) 2:4
https://doi.org/10.1007/s44357-026-00004-8

RESEARCH

Loss of brain insulin production impairs learning and memory in female mice

Stella K. Baehring[1,2,3] · Timothy P. O'Leary[1,2,3] · Haoning Howard Cen[1,2,3] · Danae Holenka[1,2,3] · Kyungchan Kim[4] · Sunday Ajayi[1,2,3] · Daniel Semenov[1,2,3] · Manuel Belmadani[5] · Hong Li[1,2,3] · Arya E. Mehran[1,2,3] · Honey Modi[1,2,3] · Melissa M. Page[6] · Søs Skovsø[7] · Paul Pavlidis[5] · Shernaz X. Bamji[1,2] · Eun-Kyoung Kim[4] · James D. Johnson[1,2,3]

Received: 18 September 2025 / Accepted: 18 February 2026

Abstract

Aims/hypothesis Diabetes is characterised by dysfunctional insulin release and action, and it is a risk factor for Alzheimer's disease, the most common form of dementia. Alterations in brain insulin signalling and metabolism have been linked with Alzheimer's disease. We hypothesised that loss of brain insulin might alter learning and memory performance.

Methods We used qPCR, immunofluorescence and western blot analysis to confirm that the ancestral insulin gene, *Ins2*, is transcribed within the brain, including in the hippocampus. To determine how locally produced insulin influences hippocampal function, we used mice with germline *Ins2* knockout ($Ins2^{-/-}$) and the normal complement of wild-type *Ins1* alleles. Compensation from the *Ins1* gene ensured normal glucose tolerance, normal insulin sensitivity, normal fasting insulin and normal body weight under these diet and housing conditions. We analysed visuo-spatial learning and memory performance using the Morris water maze. We used RNA sequencing to provide unbiased analysis of gene expression in isolated hippocampi.

Results Hippocampal *Ins2* mRNA was higher in female mice than in males, and was modulated by diet. Learning and memory were significantly impaired in female $Ins2^{-/-}$ mice relative to wild-type mice, while the performance of male $Ins2^{-/-}$ and wild-type mice did not differ. RNA sequencing showed that cyclin D1 (*Ccnd1*) was significantly reduced in $Ins2^{-/-}$ mice.

Conclusions/interpretation Our data point to female-specific roles for brain-derived *Ins2* in learning and memory function in mice.

Keywords Alzheimer's disease · Central insulin production · Hippocampus · Learning and memory

Abbreviations

NES	Normalised enrichment scores
PCA	Principal component analysis
SL	Stratum lucidum

Stella K. Baehring and Timothy P. O'Leary contributed equally to this work.

✉ James D. Johnson
James.d.johnson@ubc.ca

[1] Life Sciences Institute, University of British Columbia, Vancouver, BC, Canada

[2] Department of Cellular and Physiological Sciences, University of British Columbia, Vancouver, BC, Canada

[3] Department of Surgery, University of British Columbia, Vancouver, BC, Canada

[4] Department of Brain and Cognitive Sciences and Neurometabolomics Research Center, Daegu Gyeongbuk Institute of Science and Technology, Daegu, Republic of Korea

[5] Michael Smith Laboratories, University of British Columbia, Vancouver, BC, Canada

[6] Louvain Institute of Biomolecular Science and Technology (LIBST), Université Catholique de Louvain, Louvain-La-Neuve, Belgium

[7] Valkyrie Life Sciences, Vancouver, BC, Canada

Published online: 12 May 2026

Research in context

What is already known about this subject?

- Alzheimer's disease and type 2 diabetes share common risk factors and metabolic dysfunction
- Insulin and insulin signalling are known to have positive effects on neuronal health and cognition
- Local insulin production has been reported in the brain, including in the hippocampus, which plays critical roles in learning and memory, as well as in Alzheimer's pathophysiology

What is the key question?

- What are the consequences of deleting the *Ins2* gene, which selectively prevents local brain insulin production, on learning and memory in mice?

What are the new findings?

- Hippocampal insulin production via the *Ins2* gene is sexually dimorphic and modulated by diet
- Knocking out brain insulin production in mice does not have significant effects on glucose homeostasis in the diet and housing conditions used in this study
- Knocking out brain insulin production results in learning and memory impairments in female, but not male, mice

How might this impact on clinical practice in the foreseeable future?

- These preclinical observations demonstrate a causal role for insulin in learning and memory in female mice, but will require additional human studies before they can impact clinical practice

Introduction

Diabetes is a risk factor for dementia [1]. People living with type 2 diabetes can have cognitive impairment similar to that in early-onset Alzheimer's disease [2]. Alzheimer's disease often presents with hyperglycaemia and insulin dysfunction, including 'insulin resistance' in the brain [3–5]. Insulin enhances synaptic plasticity, promotes dendritic spine formation and increases neurotransmitter turnover [6, 7]. Insulin also influences amyloid clearance and tau phosphorylation [8]. Loss of insulin signalling in astrocytes exacerbates Alzheimer's disease pathology [9]. Evidence supporting a role for insulin in cognition in humans and preclinical models [10–12] prompted investigators to administer insulin to the brain [13] to treat cognitive dysfunction in neurodegenerative disorders. Indeed, intranasal insulin delivery improves cognitive function in patients with Alzheimer's disease [10, 13]. Lifestyle interventions that increase insulin sensitivity (e.g. diet and exercise) improve learning and memory, and are also used for Alzheimer's disease prevention and treatment [7, 14, 15].

Most studies investigating the effects of insulin in the brain are performed under the assumption that insulin in the brain is all of pancreatic origin. Although peripheral insulin crosses the blood–brain barrier via receptor-mediated transport [16], insulin is also produced locally in the brain [17]. Insulin mRNA has been measured in the choroid plexus, cerebral cortex, cerebellum and hippocampus [18–23]. The specificity of these observations has been confirmed with mice lacking the ancestral insulin 2 (*Ins2*) gene [21, 22], which survive due to the presence of the pancreas-specific insulin 1 gene (*Ins1*) [24]. We have previously shown that *Ins1* does not upregulate its gene expression in the brain to compensate for *Ins2* loss [21, 22]. Insulin synthesis has been reported in hippocampal and olfactory bulb neuronal progenitors [19, 25], which are sites of adulthood neurogenesis [26, 27]. Insulin stimulates neural stem cell survival, proliferation and differentiation [28, 29]. These and other data [19–22, 25, 30–32] clearly demonstrate that a small amount of insulin can be synthesised in the brain. Studies that include hippocampal regions consistently report elevated levels of insulin expression relative to other brain regions. The hippocampus is the main region involved in learning and memory and is one of the first to deteriorate in Alzheimer's disease. While these lines of evidence point to a role for local *Ins2* production in learning and memory [21, 25], whether brain-derived insulin directly influences learning, memory and neurogenesis has not been tested directly. In this study, we used *Ins2* knockout mice to further confirm protein insulin synthesis in the hippocampus and tested how the loss of *Ins2* influences learning and memory in both sexes.

Methods

Animals

All procedures were approved by the UBC animal care committee according to Canadian Council on Animal Care guidelines. Five-month-old C57BL/6J mice were used to assess *Ins2* expression. *Ins2* knockout mice [24] were primarily on a C57BL/6J background. *Ins2*^{GFP} knockin mice have been described previously [33]. Mice were housed in same-sex groups of two to four, in cages with a plastic dome and nesting material. In some cases, mice were singly housed due to aggression or barbering, but this did not differ between genotype or sex. Except as indicated, food and water were ad libitum. From weaning, mice were fed a chow diet (19.5 kJ/g; 25.3% energy from fat, 19.8% from protein and 54.9% from carbohydrate; 5015 Lab Diets, Richmond, USA) or a high-fat diet (23.3 kcal/g; 58.0% energy from fat, 16.4% from protein and 25.5% from carbohydrate; D12330 Open-Source Diets, New Brunswick, USA).

Immunohistochemistry and immunoblotting

Mice were perfused under isoflurane anaesthesia with phosphate-buffered saline (PBS) followed by ice-cold 4% paraformaldehyde in PBS. Brains were post-fixed in paraformaldehyde for 4 h, then cryoprotected with 30% sucrose in PBS for 48 h. Brains were embedded in OCT, frozen on dry ice and stored at − 80 °C, before sectioning at 40 µm on a cryostat. Immunostaining of dorsal hippocampal sections used rabbit anti-C-peptide (1:300; Cell Signaling Technology, 4593), rabbit anti-β-gal (1:100; Thermo Fisher Scientific, A-11132) and mouse anti-proinsulin (1:100; R&D Systems, Bio-Techne, MAB13361) primary antibodies. Donkey anti-rabbit Cy3 (1:200; Jackson ImmunoResearch, 711–165-152) and donkey anti-mouse Alexa488 (1:200; Jackson ImmunoResearch, 715–545-150) were the secondary antibodies. Hoechst 33,258 (1 µg/ml, Invitrogen, Thermo Fisher Scientific) was used to stain nuclei. Sections were cover-slipped with VECTASHIELD (Vector Laboratories) and imaged using an LSM 800 confocal microscope (Carl Zeiss).

Immunoblots of extracted proinsulin were conducted as described previously [22, 34]. Whole hippocampi of five *Ins2*$^{+/+}$ and five *Ins2*$^{-/-}$ mice were lysed and separated on 15% SDS-PAGE and blotted onto polyvinylidene difluoride membranes (Millipore, IPVH00010) for 30 min at 16 V in 25 mmol/l Tris base buffer, at pH 7.4, with 192 mmol/l glycine and 10% methanol. Membranes were blocked with 5% skim milk for 1 h and then incubated with proinsulin antibody (1:1000; Cell Signaling Technology, 8138) or GAPDH antibody (1:10,000; Cell Signaling Technology, 2118) at 4 °C overnight. After extensive washing in Tris-buffered saline with 0.1% Tween-20, the membranes were incubated with horseradish peroxidase-conjugated anti-mouse (1:3000; Cell Signaling Technology, 7076S) or anti-rabbit secondary antibody (1:10,000; Thermo, NCI1460KR).

RNA extraction, cDNA synthesis and quantitative PCR

Brain regions were dissected after CO_2 euthanasia, then snap frozen and stored at − 80°C. RNA was isolated with Trizol and chloroform followed by Qiagen RNAeasy (Thermo Fisher, 74,108). cDNA was synthesised using qScript (Quanta Bioscience, 101,414–100). Taqman real-time PCR (StepOnePlus, Applied Biosystems) used the following primers: *Ins2* Taqman reverse 280,259: GAT CTA CAA TGC CAC GCT TCT G, *Ins2* Taqman probe 224,207: CCT GCT CCC GGG CCT CCA. PCR used 2 min at 50 °C, 10 min at 95 °C, 40 15 s cycles at 95 °C and 1 min at 60°C. Samples were normalised to beta-actin (reverse log of delta). Water and cDNA from *Ins2*$^{-/-}$ tissue were negative controls.

Metabolic characterisation

Metabolic testing was performed on individual mice at multiple ages. Mice were fasted for 4 h prior to intraperitoneal injections of either glucose (4 mg/kg) or insulin (0.75 U/kg or 1.5 U/kg) in PBS. Glucose was measured in a small drop of blood sampled from the tail using OneTouch glucometers. For glucose-stimulated insulin release experiments, blood was collected from the saphenous vein following intraperitoneal injection of glucose (4 mg/kg). Insulin was quantified using an enzyme linked immunosorbent assay (ALPCO, Salem, USA). For body weight and fasting blood glucose data, some mice provided data at multiple ages. For tolerance tests and glucose-stimulated insulin secretion, data were from different cohorts of mice at each age.

Morris water maze

The Morris water maze was a white circular pool (110 cm diameter) filled with opaque 23°C water to 16 cm. The escape platform (11.5 cm diameter) was 0.5 cm below the surface. The maze was placed in a diffusely lit room with extra-maze cues. Anymaze (Stoelting) was used to record the movement of mice. Mice completed acquisition training over 6 days (four trials per day). The escape platform was located in the NW quadrant. For each trial, mice were placed into the pool at one of four release locations and were given a maximum of 60 s to reach the escape platform. Mice remained on the platform for 5–10 s before being returned to the holding cage. If mice did not reach the platform in 60 s, they were guided. The performance of mice was measured using latency to locate the escape platform, distance

travelled to reach the escape platform, cumulative search error and swim speed. Cumulative search error consisted of the total distance from the escape platform, summed across all recorded positions of the mouse (5 Hz). A correction factor was applied, where the cumulative search error value expected for the optimal swim path (determined by start location and swim speed) was subtracted from the total cumulative search error. The day following acquisition training, mice completed a 60 s probe trial without the escape platform to measure memory. The number of times mice crossed over the location of the escape platform (annulus crossings) and respective locations in other quadrants of the pool were recorded. The day following the acquisition probe, mice completed an additional day of training (acquisition retraining) to determine the extent of extinction from the probe trial, and to re-establish baseline levels of learning performance. Mice then completed reversal training to measure behavioural flexibility and the learning of a new spatial location of the escape platform. During reversal training, the escape platform was moved to the opposite side of the pool. Following reversal training, mice completed a 60 s probe trial to measure memory for the new escape platform location (SE quadrant).

Anxiety-like behaviour

The same mice tested on the Morris water maze (3 months) also completed testing for anxiety-like behaviour (4–5 months). Movements were recorded with the Ethovision (Noldus) video tracking system. Species-typical behaviours were measured with the Boris (Friad and Gamba, 2016) event scoring software. The open field consisted of a box (70 × 70 cm) made of transparent Plexiglas, with 23 cm high walls. For each trial, mice were placed into one of the four corners of the open field (pseudo-randomly determined). Locomotor activity was measured with distance travelled, while anxiety-like behaviour was assessed with entries into the centre of the open field (9th of area). Species-typical behaviours were also recorded, including number of rears, grooming duration and freezing duration. The light–dark box was constructed from Plexiglas and was divided into two chambers that were either brightly (light zone) or dimly lit (dark zone). A single light placed above the light zone provided lighting in the light–dark box and testing room. Mice were placed in the light zone facing the opening to the dark zone, and the same behavioural measures were recorded in the light–dark box, except that time in the light chamber was used as a measure of anxiety-like behaviour. The elevated-plus maze consisted of two pairs of arms, each attached to a central square. One pair of arms had opaque walls around the edge (closed arms), while the other pair of arms had no walls (open arms). A single light provided dim lighting for the elevated-plus maze and testing room. Mice were placed onto the central hub of the elevated-plus maze, facing a closed arm, and the same behavioural measurements were recorded except that time in the open arms was used as a measure of anxiety-like behaviour. The number of times that mice dipped their heads over the edge of the open arms (head-dips) was also recorded as a species-typical measure of anxiety-like behaviour. The same mice completed all three tests, with a 1 week interval between tests.

Bulk hippocampal RNA sequencing

Sample quality control was performed using the Agilent 2100 Bioanalyzer. Qualifying samples were then prepped following the standard protocol for the NEBnext Ultra ii Stranded mRNA (New England Biolabs). Sequencing was performed on the Illumina NextSeq 500 with Paired End 43 bp × 43 bp reads. Sequencing data were de-multiplexed using Illumina's bcl2fastq2. De-multiplexed read sequences were then aligned to the *Mus musculus* (PAR-masked)/mm10 reference sequence using STAR aligner. Quality control led to one outlier sample (genotype $Ins2^{-/-}$) being removed. Hierarchical clustering and principal component analysis (PCA) identified three additional outliers (one $Ins2^{+/+}$, two $Ins2^{-/-}$), which were removed. Genes with expression below 0.5 counts per million were dropped from the analysis. Differential expression analysis associated with genotype was performed using limma-trend [35] after quantile normalisation or using DESeq2 [36], which had consistent results. Pathways were analysed with clusterProfiler R using Gene Ontology (Biological Process) (FDR < 0.0001) [37] and simplify() function removed redundant GO terms (https://guangchuangyu.github.io/2015/10/use-simplify-to-remove-redundancy-of-enriched-go-terms/). Gene ratio was calculated as the number of leading-edge genes driving the enrichment divided by the total number of detected genes in each gene set. The RNA sequencing raw data are available at GEO (https://www.ncbi.nlm.nih.gov/geo/; accession number GSE305902).

Quantification of adult hippocampal neurogenesis

Twenty-month-old $Ins2^{+/+}$ and $Ins2^{-/-}$ mice were given EdU in drinking water (0.25 mg/ml) for 4 weeks. Body weight and water consumption were recorded every week. Mice were transcardially perfused with PBS (0.1 M) followed by 4% paraformaldehyde. Brains were extracted, post-fixed in 4% paraformaldehyde overnight and then transferred to a 30% sucrose solution. Brains were sliced into 40 µm coronal sections using a cryostat. EdU was detected with the Click-iT Plus EdU Alexa Fluor 647 Imaging Kit (Thermo Fisher Scientific). DCX was detected using a rabbit anti-DCX IgG polyclonal antibody (Thermo Scientific, 326 003) and a donkey anti-rabbit IgG H + L Alexa Fluor 488

secondary antibody (Invitrogen, A-21206). We used sections of intestinal villi from EdU-treated animals as positive controls for EdU labelling. Stained sections were imaged with a Zeiss LSM 880 confocal microscope (20× objective). Image stacks were stitched and maximum intensity projections were used to count EdU- and DCX-positive cells. Six sections were analysed per animal. The experimenter was blind to conditions.

Statistical analysis

For *Ins2* expression in C57BL/6J mice, data were analysed with sex as a factor when possible. $Ins2^{+/+}$ and $Ins2^{-/-}$ mice were analysed separately for each sex and age. For tolerance tests and glucose-stimulated insulin secretion, mixed-design ANOVAs (2×6 or 2×3, respectively) were used with genotype as a between-subject factor and sampling time as a within-subject factor. For acquisition and reversal training in the Morris water maze, analyses were completed separately for days 1–3 and days 4–6, which reflect initial learning and near-asymptotic performance, respectively. Measures of learning performance were analysed with mixed-design ANOVAs (2×3), using genotype as a between-subject factor and day of training as a within-subject factor. All other analyses were completed using one-way between-subject ANOVAs comparing genotypes. Post hoc tests were completed using unpaired *t* tests, with Bonferroni corrections applied independently for each statistical test. Data are expressed as mean plus or minus SEM.

Results

Ins2 is produced in the brain, expressed more in females and modulated by diet

We previously reported the presence of *Ins2* mRNA and insulin protein in the mouse brain [21], but did not show the specificity of hippocampal C-peptide and proinsulin immunoreactivity. Here, we found C-peptide, a byproduct of insulin synthesis, particularly in the dentate gyrus-CA3 (Fig. 1a). This was confirmed with immunoblots showing a small but clear *Ins2*-specific band for proinsulin in hippocampus lysates, as well as the expected prominent band in pancreas lysates (Fig. 1b). No insulin protein was found in hippocampi from $Ins2^{-/-}$ mice because the non-ancestral *Ins1* gene is not appreciably expressed in the mouse brain [21]. Proinsulin staining in the CA3 and choroid plexus was also largely absent in $Ins2^{-/-}$ mice (Fig. 1c). Importantly, in $Ins2^{+/-}$ mice, proinsulin labelling co-localised with β-gal labelling, a proxy for endogenous *Ins2* gene activity. We also visualised green fluorescence in cultured hippocampal neurons from mice with GFP knocked into the endogenous *Ins2* locus (Fig. 1d), which we have previously shown correlates with *Ins2* mRNA, pre-mRNA and protein levels in the pancreas [33]. We quantified *Ins2* mRNA across six brain regions in C57BL/6J mice. Brain *Ins2* expression was statistically different between regions ($F(5,70) = 18.42$, $p < 0.0001$), and was highest in the hippocampus and cerebellum (Fig. 2a). We observed sex differences (interaction, ($F(5,70) = 2.67$, $p < 0.05$), with females showing higher expression of *Ins2* than males in the hippocampus and cerebellum (post hoc, $p < 0.005$) (Fig. 2a). Because pancreatic *Ins2* is modulated by diet, we tested whether similar regulation occurs in the brain. In female mice, *Ins2* expression was reduced after a high-fat diet compared with a control diet (Fig. 2b). There were no differences in males, which we confirmed with an additional cohort (Fig. 2c). These data demonstrate that *Ins2* mRNA levels differ between brain regions, sexes and dietary contexts. We examined possible effects of age on brain *Ins2* mRNA in recent publicly accessible data [38], but we did not find significant differences. It should be noted that regional comparisons can be complicated by imprecise dissections and differences in cell composition, including the number of endothelial cells.

Ins1 is sufficient to preserve normal peripheral metabolism in the absence of *Ins2*

Before using $Ins2^{-/-}$ mice to examine the roles of *Ins2* in the brain, it was critical to confirm that whole body metabolism was not significantly affected. Previous studies have suggested that *Ins1* can compensate for loss of *Ins2* [21, 24, 39]. However, previous work only studied males so we characterised metabolism from 3 to 16 months of age in littermate male and female $Ins2^{-/-}$ mice side-by-side. Body weight did not differ between $Ins2^{-/-}$ and $Ins2^{+/+}$ mice at any age (Fig. 3a, b). Fasted blood glucose was similar between $Ins2^{-/-}$ and $Ins2^{+/+}$ mice (Fig. 3c, d). $Ins2^{-/-}$ and $Ins2^{+/+}$ mice did not differ in glucose tolerance or insulin tolerance tests (Fig. 3e–l). $Ins2^{-/-}$ and $Ins2^{+/+}$ mice showed statistically similar glucose-stimulated insulin secretion (Fig. 3m–p). These data suggest that *Ins1* can compensate for *Ins2* knockout under these diet and housing conditions.

Ins2 loss impairs visuo-spatial learning and memory in female, but not male, mice

Given that *Ins2* expression is prominent in the hippocampus relative to other brain regions, we examined whether hippocampal-dependent behaviour was affected by $Ins2^{-/-}$ ablation in the Morris water maze [40]. Because we observed sexual dimorphism in hippocampal *Ins2* mRNA, we compared females (Fig. 4a–f) and males (Fig. 4g–l) at 3 months of age. During acquisition training, female $Ins2^{-/-}$ and $Ins2^{+/+}$ mice did not differ in latency (Fig. 4a), distance (Fig. 4d) or cumulative search error (Fig. 4b). During the acquisition probe memory test, however, female

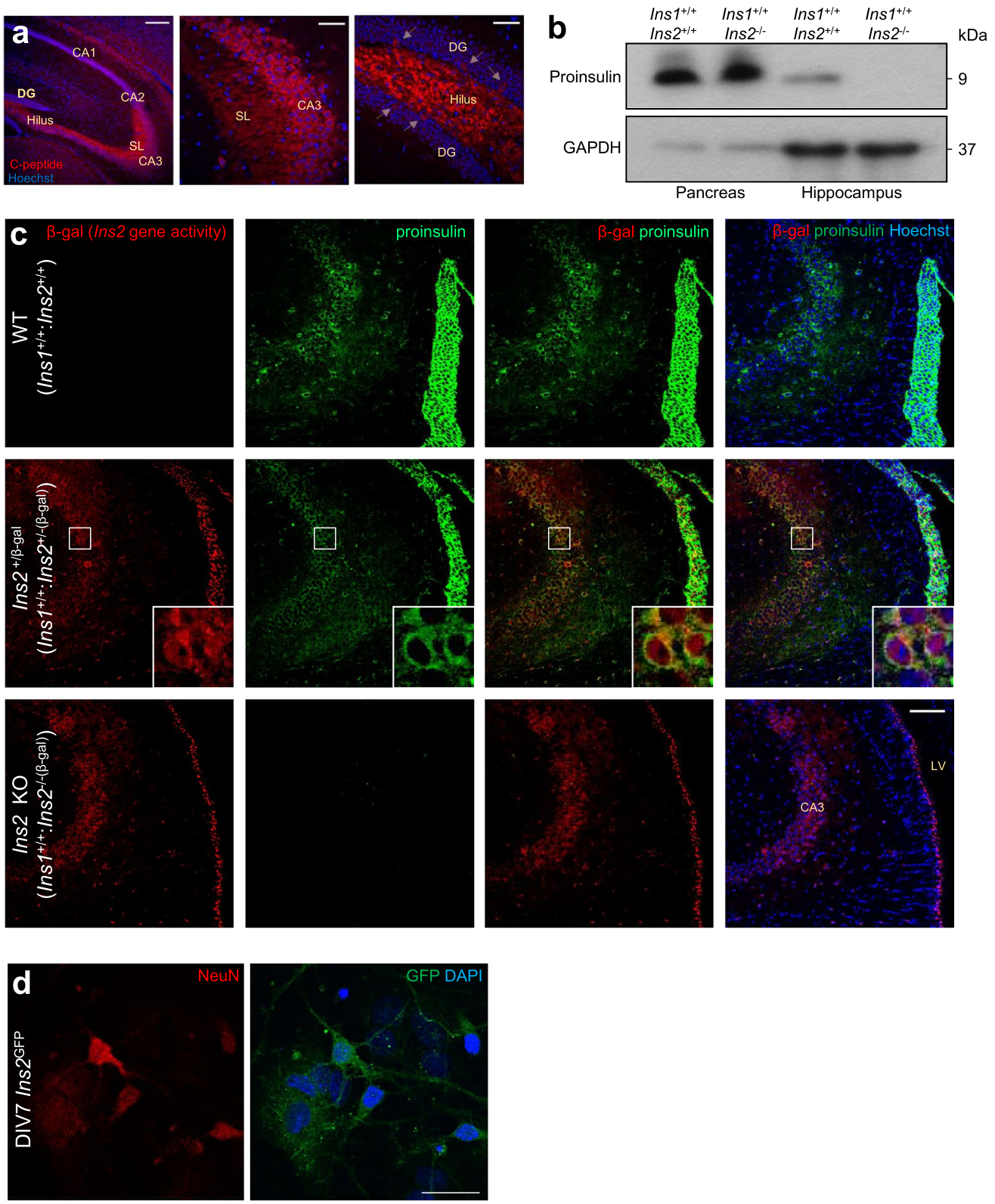

Ins2$^{-/-}$ mice completed fewer crossings over the location of the escape platform (annulus crossings) than *Ins2*$^{+/+}$ mice (Fig. 4c). We provided an additional day of acquisition training (retraining) to reduce potential extinction effects, and to provide another indirect measure of memory (assessing retention of learning performance from 2 days prior).

◂**Fig. 1** Specific *Ins2* protein immunoreactivity in mouse brain. **a** Immunoreactivity for C-peptide, a product of insulin biosynthesis, is detected in the hilus, stratum lucidum (SL), and CA3 regions of hippocampus. C-peptide-immunoreactive cells were observed in the granule cell layer of the dentate gyrus, as indicated by arrows. Scale bar, 100 µm. **b** Immunoblot of proinsulin expression in the pancreas and hippocampus from $Ins2^{+/+}$ and $Ins2^{-/-}$ mice. **c** Proinsulin-positive cells were detected and co-localised with β-galactosidase (β-gal) in the CA3 region. β-gal staining was detected in *Ins2* knockout/knockin and heterozygous mice but not in wild-type (WT) mice. Proinsulin was detected in WT and β-gal heterozygous mice but not in *Ins2* knockout mice. LV, lateral ventricle. Inset box, 20 µm. **d** GFP fluorescence in hippocampal neuron cultures of from $Ins2^{GFP/GFP}$ knockin, replacement mice. Scale bar, 10 µm. For these qualitative data, each analysis was repeated at least three times. Mice were 2–5 months of age

On the retraining day, female $Ins2^{-/-}$ mice performed worse than $Ins2^{+/+}$ mice on all measures of learning (Fig. 4a, b, d). During the first 3 days of reversal training, female $Ins2^{-/-}$ and $Ins2^{+/+}$ mice did not differ on measures of learning; over the last 3 days of reversal training, however, female $Ins2^{-/-}$ mice performed worse than $Ins2^{+/+}$ mice on all measures of learning (Fig. 4a, b, d). During the reversal probe memory test, $Ins2^{-/-}$ mice completed fewer crossings over the escape platform location than $Ins2^{+/+}$ mice (Fig. 4d). We measured swim speed throughout acquisition and reversal training, which can reflect motivation to find the platform. Female $Ins2^{-/-}$ mice swam quicker than $Ins2^{+/+}$ mice during the first 3 days of acquisition training, but this difference was not present during the last 3 days of acquisition training, nor at any point during reversal training (Fig. 4e). We conclude that differences in swim speed do not account for the impaired learning and memory observed in $Ins2^{-/-}$ mice. These results indicate impaired learning and memory in female $Ins2^{-/-}$ mice. We assessed learning and memory in male $Ins2^{-/-}$ and $Ins2^{+/+}$ mice in the Morris water maze but did not find any differences in learning performance (Fig. 4g, h, j, k, i, l). Unlike in females, loss of $Ins2^{-/-}$ in male mice did not disrupt visuo-spatial learning or memory.

Loss of *Ins2* does not influence anxiety-like behaviour or locomotor activity

The dorsal hippocampus is involved in visuo-spatial navigation and memory, while the ventral hippocampus is involved more in anxiety-like behaviour [41, 42]. We examined anxiety-like behaviour in 4–5 month old $Ins2^{-/-}$ mice using three common tests of anxiety-like behaviour: the open field, light–dark box and elevated-plus maze. All tests produced marked avoidance of anxiogenic areas, with mice spending less time in anxiogenic regions than expected by chance (see electronic supplementary material [ESM]

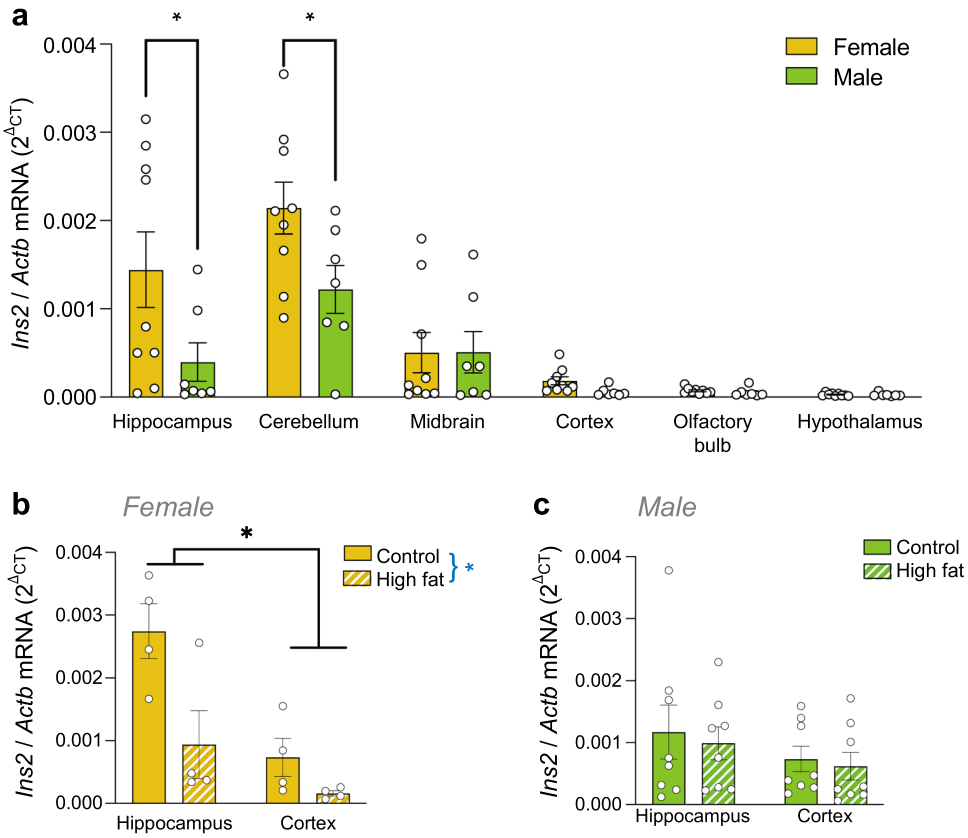

Fig. 2 *Ins2* expression in the brain is sexually dimorphic and is modulated by diet in female mice. **a** *Ins2* mRNA in male and female mice across multiple brain regions, including the hippocampus, cerebellum, cerebral cortex, olfactory bulb, hypothalamus and midbrain. *Ins2* mRNA was normalised to beta-actin mRNA. **b, c** *Ins2* mRNA in the hippocampus and cerebral cortex of male and female mice fed high-fat or control chow diets. Mice were 5 months of age. Each dot is a sample from one animal. *$p < 0.05$. In panel b, there is both a difference between brain regions, and diets

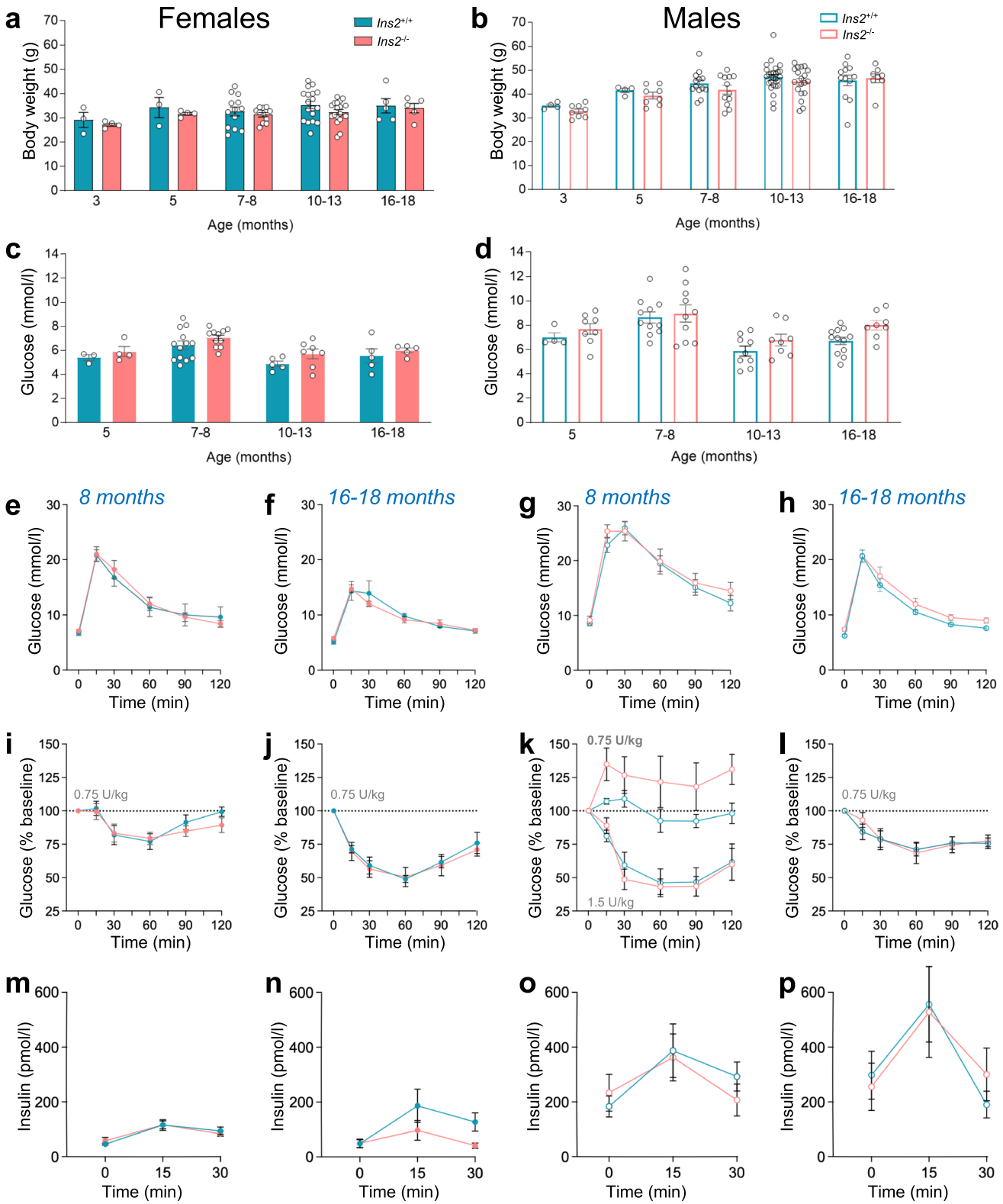

Fig. 3 Metabolic profile of young and old *Ins2*$^{-/-}$ mice on a chow diet. **a**, **b** *Ins2*$^{-/-}$ and *Ins2*$^{+/+}$ mice did not differ in body weight. **c**, **d** *Ins2*$^{-/-}$ and *Ins2*$^{+/+}$ mice did not differ in fasted blood glucose. **e**–**l** *Ins2*$^{-/-}$ and *Ins2*$^{+/+}$ mice did not differ in either glucose tolerance or insulin tolerance tests. **m**–**p** *Ins2*$^{-/-}$ and *Ins2*$^{+/+}$ mice were statistically similar in glucose-stimulated insulin secretion (16–18 months). For panels **e**–**p**, there were 4–13 mice per group. Blue closed/open circles, *Ins2*$^{+/+}$; red closed/open circles, *Ins2*$^{-/-}$

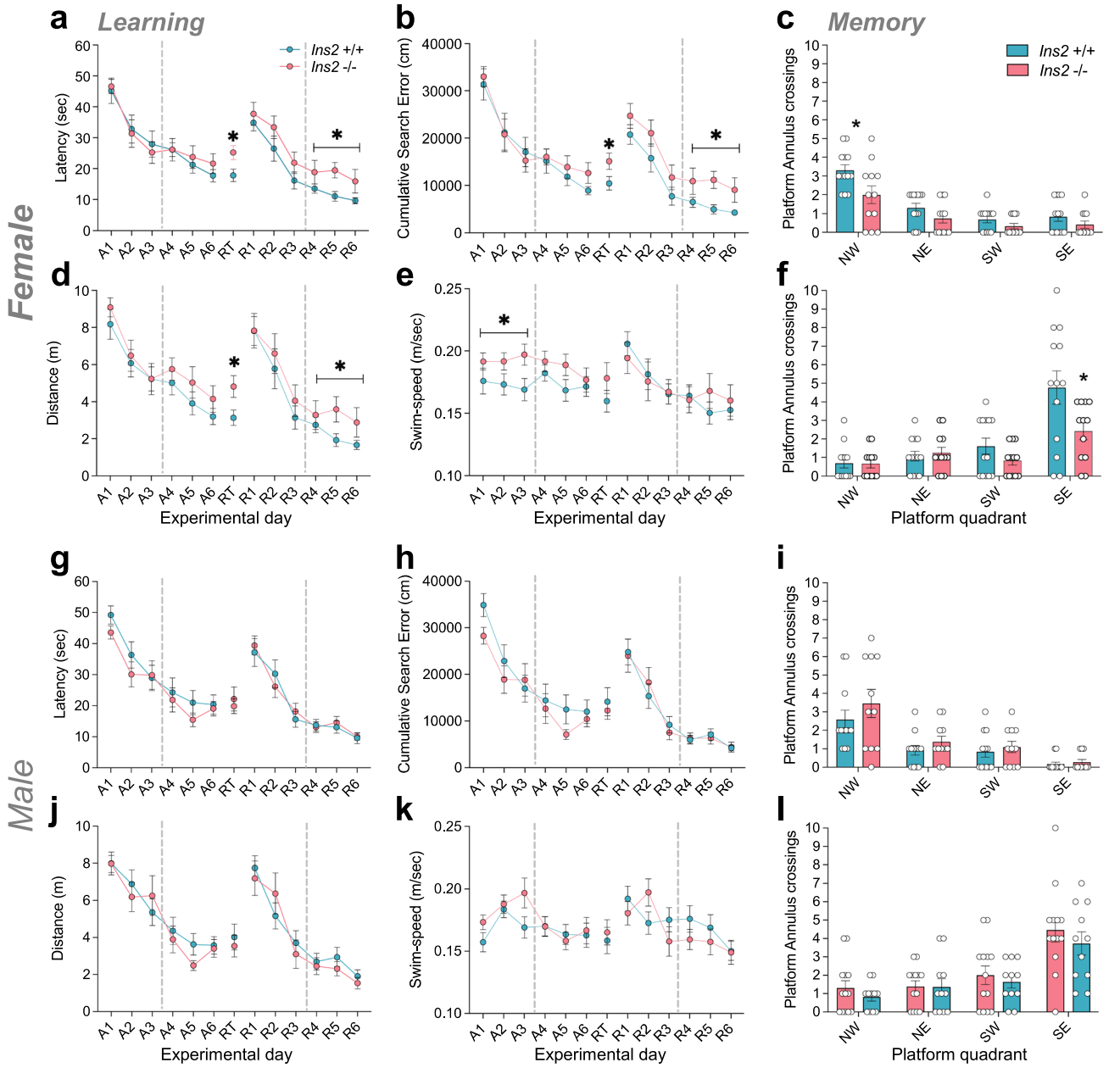

Fig. 4 Visuo-spatial learning and memory is impaired in female *Ins2*$^{-/-}$ mice. **a** Latency to locate the escape platform in female *Ins2*$^{-/-}$ mice and *Ins2*$^{+/+}$ mice during acquisition (A1–6), retraining (RT) and reversal training (R1–6). Performance for the first 3 days and last 3 days of acquisition and reversal training were analysed separately (indicated by vertical dashed line). **b** Cumulative search error for female *Ins2*$^{-/-}$ and *Ins2*$^{+/+}$ mice on the same study days. **c** Platform annulus crossings completed by female *Ins2*$^{-/-}$ and *Ins2*$^{+/+}$ mice during the acquisition probe trial. **d** Distance travelled by female *Ins2*$^{-/-}$ and *Ins2*$^{+/+}$ mice to reach the escape platform on each study day. **e** Swim speed for female *Ins2*$^{-/-}$ and *Ins2*$^{+/+}$ mice over acquisition and reversal training. **f** Platform annulus crossings during the reversal probe trial. Panels **g–l** Show the same measurements as above, but for male mice. Mice were 3 months of age, 11–13 mice per group. $^{*}p < 0.05$

Fig. 1). For both males and females, however, *Ins2*$^{-/-}$ and *Ins2*$^{+/+}$ mice did not differ in anxiety-related behaviour. We also extended our analysis to include locomotor activity and species-typical measures of exploration and anxiety-like behaviour (e.g. grooming, rearing and freezing), but did not find any differences between *Ins2*$^{-/-}$ and *Ins2*$^{+/+}$ mice (ESM Fig. 1). Therefore, among the behaviours we studied, the effects of *Ins2* knockout in female mice appear to be specific to learning and memory in the Morris water maze.

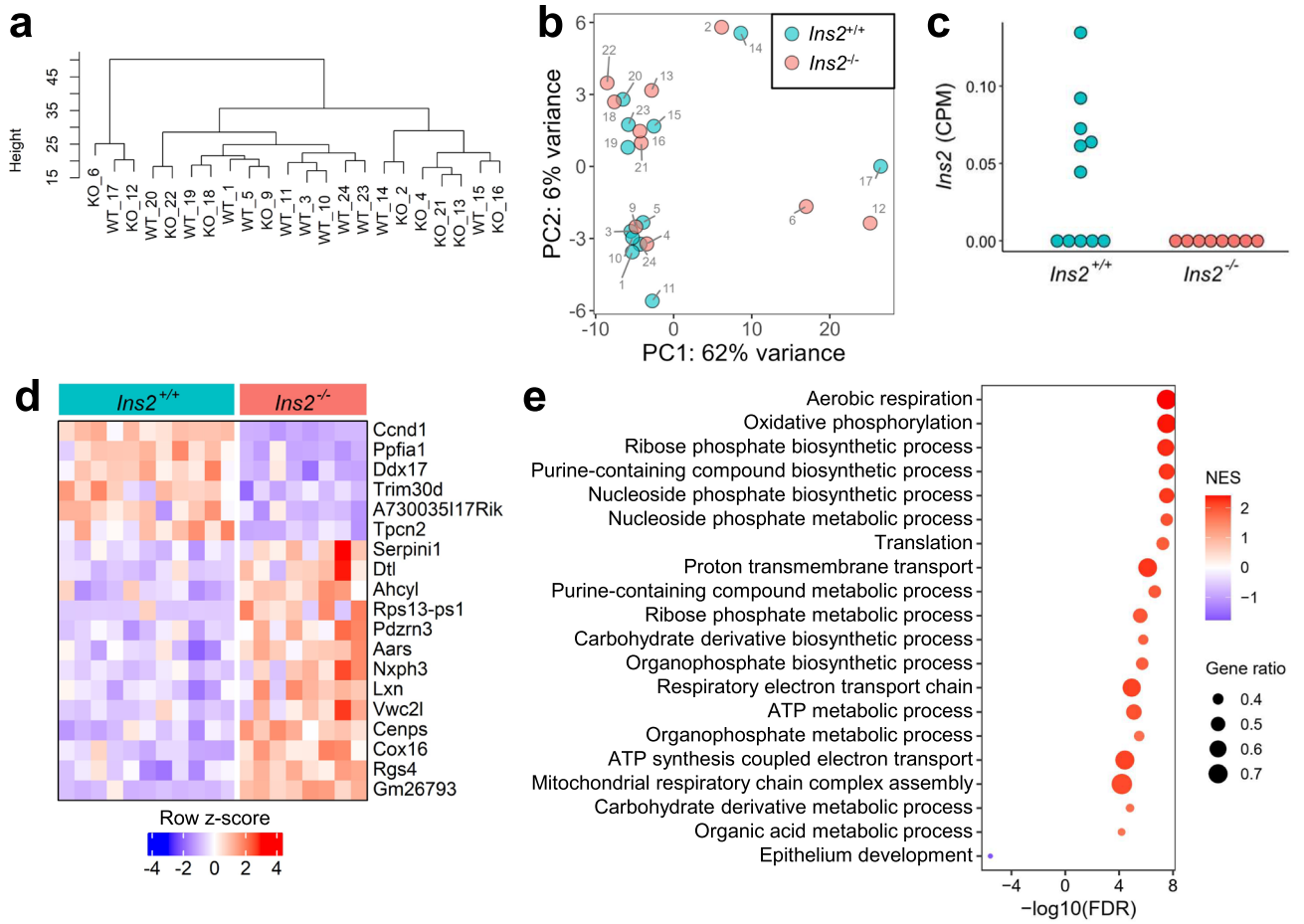

Fig. 5 Bulk mRNA sequencing and cluster analysis of isolated *Ins2*$^{-/-}$ and *Ins2*$^{+/+}$ hippocampi from female mice. **a** Cluster dendrogram reflects a measure of the distance between samples (height). **b** PCA showing the three outlier samples (6, 12 and 17). **c** No *Ins2* mRNA was detected in *Ins2*.$^{-/-}$ hippocampi. **d** Differentially expressed genes ranked from most significantly downregulated to upregulated (top to bottom). **e** Gene set enrichment analysis using Gene Ontology (Biological Process) shows the normalised enrichment scores (NES; FDR < 0.0001)

Transcriptomics of hippocampi from aged female *Ins2*$^{-/-}$ mice

We conducted bulk hippocampal RNA-seq in female *Ins2*$^{-/-}$ mice (12 months) to identify long-standing molecular mechanisms associated with defects in learning and memory. We started with 11 samples in each group, but three samples (6, 12 and 17) were removed because they were outliers based on hierarchical clustering and PCA (Fig. 5a,b). *Ins2* mRNA was absent in *Ins2*$^{-/-}$ samples (Fig. 5c). We identified six downregulated and 13 upregulated genes in *Ins2*$^{-/-}$mice (Fig. 5d). The cell cycle regulatory gene *Ccnd1* and the stem cell regulatory long noncoding RNA Gm26793 [43] were the most significantly downregulated and upregulated genes, respectively. These genes were robustly altered even when the outlier samples were included. Gene set enrichment analysis showed that the (semi-redundant) Gene Ontology terms 'aerobic respiration' and 'oxidative phosphorylation' were the most significantly upregulated (Fig. 5e). Insulin regulates oxidative phosphorylation in many tissues, including the brain [44]. The Gene Ontology term 'epithelium development' was the only significantly downregulated pathway (Fig. 5e). These relatively well-powered transcriptomic studies point to potential molecular mechanisms underlying the effects of insulin signalling in the female rodent hippocampus.

Neurogenesis in *Ins2*$^{-/-}$ mice

Given that 1-year-old *Ins2*$^{-/-}$ mice had reduced *Ccnd1* mRNA, a gene with roles in neurogenesis, we investigated whether hippocampal neurogenesis was altered in *Ins2*$^{-/-}$ mice (> 1 year old). We first confirmed the robustness of our staining by confirming Edu-positive cells in intestinal villi, a region with high cell proliferation (ESM Fig. 2a). In female brains, the densities of Edu-positive cells

and DCX-positive cells did not differ between *Ins2*$^{-/-}$ and *Ins2*$^{+/+}$ mice (ESM Fig. 2b–f). In male brains, *Ins2*$^{-/-}$ mice had a larger density of EdU-positive cells in the dorsal ($F(1,10) = 5.57$, $p < 0.05$)(ESM Fig. 2c), but not ventral, hippocampus (ESM Fig. 2d). We have shown that reducing *Ins2* has cell-autonomous proliferative effects in pancreatic beta cells [45]. One could speculate that this compensation may have prevented male *Ins2*$^{-/-}$ mice from developing deficits in learning and memory. The density of DCX-positive cells did not differ between *Ins2*$^{-/-}$ and Ins2$^{+/+}$ male mice in either the dorsal or ventral hippocampus (ESM Fig. 2e,f). These data suggest that adult hippocampal neurogenesis, measured at this stage of life, is not a major factor in differences in learning and memory in female *Ins2*$^{-/-}$ mice, but additional studies in younger mice should be conducted before this mechanism can be ruled out.

Discussion

The objectives of this study were to further elucidate the expression of insulin in the hippocampus and to determine the role of brain-produced insulin on hippocampus-dependent learning and memory. This type of loss-of-function causality study cannot be conducted in humans. Given that *Ins2* is expressed in both the brain and pancreas, it was important to confirm that *Ins2* knockout did not alter peripheral metabolism, which could theoretically affect brain function indirectly. Using mice devoid of hippocampal proinsulin we defined a female-specific role for brain insulin production in learning and memory. To the best of our knowledge, this is the first time mammalian cognitive behaviour has been examined in the context of genetic insulin reduction. We found sexual dimorphic *Ins2* expression and environmental modulation in the hippocampus, as well as female-specific consequences of *Ins2* loss. Women are at higher risk of developing early-onset Alzheimer's disease [46]. The female-specific memory impairment observed after loss of *Ins2* highlights the importance of including females in preclinical research regarding insulin and cognitive dysfunction, and predicts that insulin administration may be more effective at treating cognitive impairment in females than males. Importantly, compared with other studies in young mice, our RNA-seq experiment was conducted on middle-aged mice, which is especially relevant to understanding the potential role of *Ins2* in the development of mild-cognitive impairment and early-onset Alzheimer's disease.

Previous studies have ablated insulin-expressing neurons with the beta cell toxin streptozocin [47–49], but such drugs may affect other areas of the body and brain. Although the present study circumvents some of these issues, the *Ins2* knockout model has limitations. While we observed a female-specific effect, we have no information on the oestrous status of these mice during the behavioural studies. With a global *Ins2* knockout, it cannot be concluded that the results of this study are exclusively due to brain insulin loss. Generating tissue-specific *Ins2* knockout could circumvent this limitation, but our efforts to do so have been unsuccessful. In addition, the loss of *Ins2* was lifelong, and thus effects of *Ins2* loss during early development cannot be excluded. Future studies could employ a floxed *Ins2* allele and an inducible brain-specific Cre driver to selectively knock out *Ins2* during adulthood. Another limitation of our work is that the behavioural, RNA-seq and neurogenesis experiments were conducted at different ages, which may limit our ability to resolve mechanisms for *Ins2* in hippocampal-dependent memory. Our work also does not identify the cellular target(s) of local insulin production, nor their molecular mechanisms. Insulin receptors have been shown to mediate important roles of insulin in many neuronal cell populations in the brain, including the hippocampus [50–52]. Insulin also acts directly through insulin receptors to modulate the activity of non-neuronal brain cells including astrocytes [53–55]. Loss of insulin action in astrocytes significantly worsened Alzheimer's pathologies in a mouse model [9]. Cerebrovascular insulin receptors were also shown to be deficient in Alzheimer's disease [56]. More research is required to elucidate local insulin–insulin receptor trophic circuits across cell types in the brain, including in humans.

Supplementary Information The online version contains supplementary material available at https://doi.org/10.1007/s44357-026-00004-8.

Acknowledgements We thank many colleagues for helpful discussions. Components of this work can also be found in SKB's MSc thesis.

Author contributions SKB designed studies, performed experiments, analysed and interpreted data and co-wrote the manuscript. TPO designed studies, performed experiments, analysed and interpreted data and co-wrote the manuscript. HHC analysed bioinformatic data and helped write the manuscript. DH performed experiments and analysed and interpreted data. KK performed experiments. SA performed experiments. DS performed experiments. MB analysed bioinformatic data. HL performed experiments. AEM performed experiments and analysed and interpreted data. HM performed experiments and analysed and interpreted data. MMP performed experiments and analysed and interpreted data. SS performed experiments and analysed and interpreted data. PP supported bioinformatic studies, interpreted data and edited the manuscript. SXB designed studies, interpreted data and edited the manuscript. E-KK analysed data and provided a key reagent. JDJ conceived the project, designed and interpreted studies, co-wrote the manuscript and is the guarantor of this work. All authors reviewed and approved the final version.

Funding This work was supported by a Brain Canada Multi-Investigator grant to JDJ, SXB and PP.

Data availability RNA sequencing data are available at GEO ([https://www.ncbi.nlm.nih.gov/geo/]; accession number GSE305902). Other data can be shared on request without restriction after contacting the corresponding author.

Declarations

Competing interests The authors declare no competing interests.

References

1. Hölscher C (2011) Diabetes as a risk factor for Alzheimer's disease: insulin signalling impairment in the brain as an alternative model of Alzheimer's disease. Biochem Soc Trans 39(4):891–897. https://doi.org/10.1042/BST0390891
2. Ryan CM, Geckle M (2000) Why is learning and memory dysfunction in Type 2 diabetes limited to older adults? Diabetes Metab Res Rev 16(5):308–315. https://doi.org/10.1002/1520-7560(2000)9999:9999<::AID-DMRR141>3.0.CO;2-X
3. De Felice FG, Lourenco MV, Ferreira ST (2014) How does brain insulin resistance develop in Alzheimer's disease? Alzheimers Dement 10(1):S26–S32. https://doi.org/10.1016/j.jalz.2013.12.004
4. Talbot K, Wang H-Y, Kazi H et al (2012) Demonstrated brain insulin resistance in Alzheimer's disease patients is associated with IGF-1 resistance, IRS-1 dysregulation, and cognitive decline. J Clin Invest 122(4):1316–1338. https://doi.org/10.1172/jci59903
5. Ma L, Wang J, Li Y (2015) Insulin resistance and cognitive dysfunction. Clin Chim Acta 444:18–23. https://doi.org/10.1016/j.cca.2015.01.027
6. Forner S, Baglietto-Vargas D, Martini AC, Trujillo-Estrada L, LaFerla FM (2017) Synaptic impairment in Alzheimer's disease: a dysregulated symphony. Trends Neurosci 40(6):347–357. https://doi.org/10.1016/j.tins.2017.04.002
7. Kellar D, Craft S (2020) Brain insulin resistance in Alzheimer's disease and related disorders: mechanisms and therapeutic approaches. Lancet Neurol 19(9):758–766. https://doi.org/10.1016/S1474-4422(20)30231-3
8. Laws SM, Gaskin S, Woodfield A et al (2017) Insulin resistance is associated with reductions in specific cognitive domains and increases in CSF tau in cognitively normal adults. Sci Rep 7(1):1–11. https://doi.org/10.1038/s41598-017-09577-4
9. Chen W, Huang Q, Lazdon EK et al (2023) Loss of insulin signaling in astrocytes exacerbates Alzheimer-like phenotypes in a 5xFAD mouse model. Proc Natl Acad Sci U S A 120(21):e2220684120. https://doi.org/10.1073/pnas.2220684120
10. Freiherr J, Hallschmid M, Frey WH et al (2013) Intranasal insulin as a treatment for Alzheimer's disease: a review of basic research and clinical evidence. CNS Drugs 27(7):505–514. https://doi.org/10.1007/s40263-013-0076-8
11. Zhang H, Hao Y, Manor B et al (2015) Intranasal insulin enhanced resting-state functional connectivity of hippocampal regions in type 2 diabetes. Diabetes 64(3):1025–1034. https://doi.org/10.2337/db14-1000
12. Li X, Yang Y, Bai X et al (2024) A brain-derived insulin signal encodes protein satiety for nutrient-specific feeding inhibition. Cell Rep 43(6):114282. https://doi.org/10.1016/j.celrep.2024.114282
13. Born J, Lange T, Kern W, McGregor GP, Bickel U, Fehm HL (2002) Sniffing neuropeptides: a transnasal approach to the human brain. Nat Neurosci 5(6):514–516. https://doi.org/10.1038/nn0602-849
14. Ko Y, Chye SM (2020) Lifestyle intervention to prevent Alzheimer's disease. Rev Neurosci 31(8):817–824. https://doi.org/10.1515/revneuro-2020-0072
15. Braak H, Braak E (1995) Staging of Alzheimer's disease-related neurofibrillary changes. Neurobiol Aging 16(3):271–278. https://doi.org/10.1016/0197-4580(95)00021-6
16. Gray SM, Aylor KW, Barrett EJ (2017) Unravelling the regulation of insulin transport across the brain endothelial cell. Diabetologia 60(8):1512–1521. https://doi.org/10.1007/s00125-017-4285-4
17. Dakic T, Jevdjovic T, Lakic I et al (2023) The expression of insulin in the central nervous system: what have we learned so far? Int J Mol Sci 24(7):6586. https://doi.org/10.3390/ijms24076586
18. Molnar G, Farago N, Kocsis AK et al (2014) GABAergic neurogliaform cells represent local sources of insulin in the cerebral cortex. J Neurosci 34(4):1133–1137. https://doi.org/10.1523/JNEUROSCI.4082-13.2014
19. Nemoto T, Toyoshima-Aoyama F, Yanagita T et al (2014) New insights concerning insulin synthesis and its secretion in rat hippocampus and cerebral cortex: amyloid-beta1-42-induced reduction of proinsulin level via glycogen synthase kinase-3beta. Cell Signal 26(2):253–259. https://doi.org/10.1016/j.cellsig.2013.11.017
20. Mazucanti CH, Liu QR, Lang D et al (2019) Release of insulin produced by the choroid plexis is regulated by serotonergic signaling. JCI Insight. https://doi.org/10.1172/jci.insight.131682
21. Mehran AE, Templeman NM, Brigidi GS et al (2012) Hyperinsulinemia drives diet-induced obesity independently of brain insulin production. Cell Metab 16(6):723–737. https://doi.org/10.1016/j.cmet.2012.10.019
22. Lee J, Kim K, Cho JH et al (2020) Insulin synthesized in the paraventricular nucleus of the hypothalamus regulates pituitary growth hormone production. JCI Insight. https://doi.org/10.1172/jci.insight.135412
23. Mazucanti CH, Kennedy V Jr., Premathilake HU et al (2023) AAV5-mediated manipulation of insulin expression in choroid plexus has long-term metabolic and behavioral consequences. Cell Rep 42(8):112903. https://doi.org/10.1016/j.celrep.2023.112903
24. Duvillie B, Cordonnier N, Deltour L et al (1997) Phenotypic alterations in insulin-deficient mutant mice. Proc Natl Acad Sci USA 94(10):5137–5140. https://doi.org/10.1073/pnas.94.10.5137
25. Kuwabara T, Kagalwala MN, Onuma Y et al (2011) Insulin biosynthesis in neuronal progenitors derived from adult hippocampus and the olfactory bulb. EMBO Mol Med 3(12):742–754. https://doi.org/10.1002/emmm.201100177
26. Berdugo-Vega G, Dhingra S, Calegari F (2023) Sharpening the blades of the dentate gyrus: how adult-born neurons differentially modulate diverse aspects of hippocampal learning and memory. EMBO J 42(22):e113524. https://doi.org/10.15252/embj.202313524
27. Hitoshi S, Mandyam CD, Shetty AK (2023) Editorial: Advances in adult neurogenesis. Front Neurosci 17:1307844. https://doi.org/10.3389/fnins.2023.1307844
28. Brooker GJ, Kalloniatis M, Russo VC, Murphy M, Werther GA, Bartlett PF (2000) Endogenous IGF-1 regulates the neuronal differentiation of adult stem cells. J Neurosci Res 59(3):332–341. https://doi.org/10.1002/(sici)1097-4547(20000201)59:3<332::aid-jnr6>3.0.co;2-2
29. Åberg MA, Åberg ND, Palmer TD et al (2003) IGF-I has a direct proliferative effect in adult hippocampal progenitor cells. Mol Cell

Neurosci 24(1):23–40. https://doi.org/10.1016/S1044-7431(03)00082-4
30. Young IIIWS (1986) Periventricular hypothalamic cells in the rat brain contain insulin mRNA. Neuropeptides 8(2):93–97. https://doi.org/10.1016/0143-4179(86)90035-1
31. Havrankova J, Schmechel D, Roth J, Brownstein M (1978) Identification of insulin in rat brain. Proc Natl Acad Sci USA 75(11):5737–5741. https://doi.org/10.1073/pnas.75.11.5737
32. Csajbok EA, Tamas G (2016) Cerebral cortex: a target and source of insulin? Diabetologia 59(8):1609–1615. https://doi.org/10.1007/s00125-016-3996-2
33. Chu CMJ, Modi H, Ellis C et al (2022) Dynamic Ins2 gene activity defines beta-cell maturity states. Diabetes 71(12):2612–2631. https://doi.org/10.2337/db21-1065
34. Kim S, Kim N, Park S et al (2020) Tanycytic TSPO inhibition induces lipophagy to regulate lipid metabolism and improve energy balance. Autophagy 16(7):1200–1220. https://doi.org/10.1080/15548627.2019.1659616
35. Ritchie ME, Phipson B, Wu D et al (2015) Limma powers differential expression analyses for RNA-sequencing and microarray studies. Nucleic Acids Res 43(7):e47–e47. https://doi.org/10.1093/nar/gkv007
36. Love MI, Huber W, Anders S (2014) Moderated estimation of fold change and dispersion for RNA-seq data with DESeq2. Genome Biol 15(12):550. https://doi.org/10.1186/s13059-014-0550-8
37. Yu G, Wang LG, Han Y, He QY (2012) ClusterProfiler: an R package for comparing biological themes among gene clusters. OMICS 16(5):284–287. https://doi.org/10.1089/omi.2011.0118
38. Kumar NH, Kluever V, Barth E et al (2024) Comprehensive transcriptome analysis reveals altered mRNA splicing and post-transcriptional changes in the aged mouse brain. Nucleic Acids Res 52(6):2865–2885. https://doi.org/10.1093/nar/gkae172
39. Leroux L, Desbois P, Lamotte L et al (2001) Compensatory responses in mice carrying a null mutation for Ins1 or Ins2. Diabetes 50(Suppl 1):S150-153. https://doi.org/10.2337/diabetes.50.2007.s150
40. D'Hooge R, De Deyn PP (2001) Applications of the Morris water maze in the study of learning and memory. Brain Res Brain Res Rev 36(1):60–90. https://doi.org/10.1016/s0165-0173(01)00067-4
41. Bannerman DM, Grubb M, Deacon RM, Yee BK, Feldon J, Rawlins JN (2003) Ventral hippocampal lesions affect anxiety but not spatial learning. Behav Brain Res 139(1–2):197–213. https://doi.org/10.1016/s0166-4328(02)00268-1
42. Fanselow MS, Dong HW (2010) Are the dorsal and ventral hippocampus functionally distinct structures? Neuron 65(1):7–19. https://doi.org/10.1016/j.neuron.2009.11.031
43. Liu Z, Wan X, Chen J et al (2025) Genomic locus of lncRNA-Gm26793 forms an inter-chromosomal interaction with Cubn to ensure proper stem cell differentiation in vitro and in vivo. Cell Discovery 11(1):53. https://doi.org/10.1038/s41421-025-00805-0
44. Milstein JL, Ferris HA (2021) The brain as an insulin-sensitive metabolic organ. Mol Metab 52:101234. https://doi.org/10.1016/j.molmet.2021.101234
45. Szabat M, Page MM, Panzhinskiy E et al (2016) Reduced insulin production relieves endoplasmic reticulum stress and induces β cell proliferation. Cell Metab 23(1):179–193. https://doi.org/10.1016/j.cmet.2015.10.016
46. Neu SC, Pa J, Kukull W et al (2017) Apolipoprotein E genotype and sex risk factors for Alzheimer disease: a meta-analysis. JAMA Neurol 74(10):1178–1189. https://doi.org/10.1001/jamaneurol.2017.2188
47. Grünblatt E, Salkovic-Petrisic M, Osmanovic J, Riederer P, Hoyer S (2007) Brain insulin system dysfunction in streptozotocin intracerebroventricularly treated rats generates hyperphosphorylated tau protein. J Neurochem 101(3):757–770. https://doi.org/10.1111/j.1471-4159.2006.04368.x
48. Plaschke K, Kopitz J, Siegelin M et al (2010) Insulin-resistant brain state after intracerebroventricular streptozotocin injection exacerbates Alzheimer-like changes in Tg2576 AβPP-overexpressing mice. J Alzheimers Dis 19(2):691–704. https://doi.org/10.3233/JAD-2010-1270
49. Lester-Coll N, Rivera EJ, Soscia SJ, Doiron K, Wands JR, de la Monte SM (2006) Intracerebral streptozotocin model of type 3 diabetes: relevance to sporadic Alzheimer's disease. J Alzheimers Dis 9(1):13–33. https://doi.org/10.3233/jad-2006-9102
50. Chen W, Cai W, Hoover B, Kahn CR (2022) Insulin action in the brain: cell types, circuits, and diseases. Trends Neurosci 45(5):384–400. https://doi.org/10.1016/j.tins.2022.03.001
51. Dixon-Salazar TJ, Fourgeaud L, Tyler CM, Poole JR, Park JJ, Boulanger LM (2014) MHC class I limits hippocampal synapse density by inhibiting neuronal insulin receptor signaling. J Neurosci 34(35):11844–11856. https://doi.org/10.1523/jneurosci.4642-12.2014
52. Soto M, Cai W, Konishi M, Kahn CR (2019) Insulin signaling in the hippocampus and amygdala regulates metabolism and neurobehavior. Proc Natl Acad Sci USA 116(13):6379–6384. https://doi.org/10.1073/pnas.1817391116
53. Cai W, Xue C, Sakaguchi M et al (2018) Insulin regulates astrocyte gliotransmission and modulates behavior. J Clin Invest 128(7):2914–2926. https://doi.org/10.1172/jci99366
54. Taib B, Deme P, Gupta S et al (2025) Insulin acts on astrocytes to shift their substrate preference to fatty acids. iScience 28(4):111642. https://doi.org/10.1016/j.isci.2024.111642
55. Fernandez AM, Martinez-Rachadell L, Navarrete M et al (2022) Insulin regulates neurovascular coupling through astrocytes. Proc Natl Acad Sci USA 119(29):e2204527119. https://doi.org/10.1073/pnas.2204527119
56. Leclerc M, Bourassa P, Tremblay C et al (2022) Cerebrovascular insulin receptors are defective in Alzheimer's disease. Brain 146(1):75–90. https://doi.org/10.1093/brain/awac309